JOURNAL OF MATERIALS SCIENCE **40** (2005) 2875–2882

Using hybrid reinforcement methodology to enhance overall mechanical performance of pure magnesium

W. L. E. WONG, M. GUPTA*
Department of Mechanical Engineering, National University of Singapore, 9 Engineering Drive 1, Singapore 117576
E-mail: mpegm@nus.edu.sg

In the present study, magnesium based composites containing galvanised iron wire mesh and carbon fibres as continuous reinforcement were fabricated using the disintegrated melt deposition technique followed by hot extrusion. Microstructural characterisation of the extruded composite samples showed minimal porosity and good interfacial integrity between iron wire mesh and the matrix. The penetration of magnesium in between carbon fibres remains limited. Mechanical characterization revealed that the addition of reinforcements lead to an increase in hardness, dynamic modulus and 0.2%YS, did not affect the UTS and reduced the ductility. The overall mechanical performance of the composite with hybrid reinforcement synthesized in this study remained superior when compared to conventional composite formulations with comparatively higher volume fraction of reinforcement.

1. Introduction

Increasing demand and application of novel composite materials into realistic engineering components, such as electronic heat sinks, automotive drive shafts, jet fighter aircraft fins or combustion engine components have led to intensive research efforts into the design and development of metal matrix composites [1]. The greatest advantage of MMCs lies in the large variety of possible matrices and reinforcements and the vast combinations and fabrication routes available. Thus, specific material properties can be tailored to meet the specific and challenging end service requirements [1]. So far most of the research is focused on MMCs based on light metals like magnesium, aluminium and titanium in order to minimize weight. In addition, iron, copper and nickel-based superalloys have also been used as matrix materials in certain applications [2]. Magnesium and its alloys are excellent candidates for weight critical applications because of their significantly low density (density of 1.74 g/cm^3 compared to 2.7 g/cm^3 for aluminium and 4.5 g/cm^3 for titanium). However, the use of magnesium and its alloys in engineering applications is often limited by its inferior elastic modulus and corrosion resistance.

In recent years, several research attempts are made to study: (a) the processing methodologies to fabricate magnesium based composites [3–11], (b) effects of matrix constitution on the microstructure and properties of end composites [3–11], (c) effects of different kind of reinforcement on the microstructure and properties [3–15], and (d) reinforcement/matrix interfacial characteristics on the mechanical properties [10–20]. Most of these research attempts were limited to the metal matrix composites with only one type of reinforcement. Very limited studies have been conducted by researchers [21, 22] to investigate the effect of the presence of two types of reinforcement on the mechanical properties. These studies involved the use of fibre and particle combinations in volume fraction exceeding 0.25 and using pressure infiltration technique. No studies have been made so far to investigate the effect of two types of reinforcements that are either continuous or continuous/interconnected in nature and in low volume fraction (<5 volume percent) on the physical and mechanical properties of pure magnesium.

Accordingly, the aim of the present work was to synthesise a novel hybrid composite containing two types of continuous reinforcement using the cost effective and environmental friendly disintegrated melt deposition technique followed by hot extrusion. The term 'hybrid composite' is used to describe composites containing more than one type of reinforcement [21–23]. Hybrid composites are attractive structural materials because they can provide an added degree of freedom of tailoring composites and achieving properties that cannot be realised in single reinforcement composite systems. Hybridization allows the combination of more expensive fibres (in this case carbon fibres) with inexpensive iron mesh with the potential of balancing the stiffness, strength, ductility and other material

*Author to whom all correspondence should be addressed.

properties [23]. The synthesized materials were examined in terms of microstructure, physical and mechanical properties. Particular emphasis was placed to rationalize the improvement in physical and mechanical properties of elemental magnesium with the presence of two types of continuous reinforcement in lower volume fraction range (<5 volume percent).

2. Experimental procedures

2.1. Materials

In this study, magnesium turnings of 99.9+% purity were utilized as the matrix material. Galvanized iron mesh of 0.71 mm diameter with an equivalent of 10.8-vol.% zinc in the form of coating was used as one of the reinforcement. The mesh opening was 0.7 cm × 0.7 cm. The other reinforcement consists of Hexcel IM7 (HS-CP-5000) PAN-based carbon fibres of 6000 filament count tows with properties as follows: density 1.78 g/cm^3, filament diameter of 5.2 microns, tensile strength 5175 MPa, tensile modulus 276 GPa and ultimate elongation of 1.87% [24]. Galvanized iron mesh in the form of 3 concentric rings of different diameter was fabricated (see Fig. 1a). The mesh was first cut into smaller rectangle pieces and rolled to form a cylindrical form. The ends of the cylinder were mechanically interlocked. Carbon fibres were wound around the iron mesh in a helical manner on the innermost ring of 10 mm diameter as shown in Fig. 1b.

2.2. Processing

The composites were synthesized using the disintegrated melt deposition (DMD) technique [25–27]. The magnesium turnings were superheated to 750°C in a graphite crucible under an inert argon atmosphere. The reinforcements were aligned inside a steel mould of 40 mm diameter located below the crucible. Upon reaching the superheat temperature, the molten metal was stirred at a speed of approximately 450 rpm for 5 min using a twin blade (pitch 45°) mild steel impeller coated with Zirtex-25 (86% ZrO_2, 8.8% Y_2O_3, 3.6% SiO_2, 1.2% K_2O and Na_2O and 0.3% trace organics) to avoid possible iron contamination. The melt was then released through a 10 mm hole at the base of the crucible and was disintegrated by two jets of argon gas as it enters the mould. The argon gas flow rate was maintained at 25 l/min. Similar parameters were used for synthesizing pure magnesium, except that no reinforcement preform was placed in the mould. The deposited ingots were machined down to a diameter of 35 mm and then hot extruded at 350°C employing an extrusion ratio of approximately 20:1. The ingots were heated at 400°C for an hour in a constant temperature furnace before extrusion.

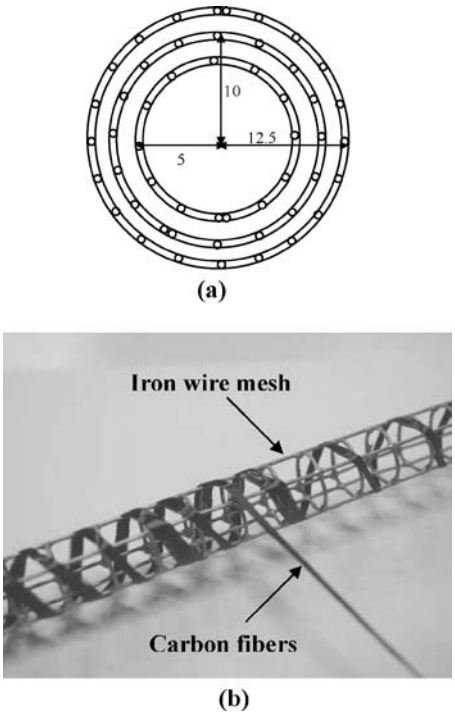

Figure 1 (a) Planar view of mesh structure, and (b) tying of carbon fibers around mesh structure.

2.3. Density measurement

The densities of the monolithic and composite samples were measured in accordance with Archimedes principle [28]. The density measurements involved weighing polished samples in air and when immersed in distilled water. The samples were weighed using an AND HM-202 electronic balance with an accuracy of ±0.0001 g.

2.4. Microstructural characterization

Microstructural characterization was conducted on the extruded samples in order to determine the presence of micropores, grain morphology and interfacial integrity between the reinforcements and matrix. The grain size and grain morphology were determined by image analysis of the representative micrographs taken using an optical microscope. The optical micrographs were analyzed using the Scion Image Analyzer software and compared with ASTM E112-96 to obtain the corresponding ASTM grain size number. A JEOL JSM-5600LV SEM equipped with energy dispersive X-Ray spectrometer (EDX) was used to investigate the interfacial integrity between the reinforcements and the matrix, the presence of porosity and interfacial reactions. EDX was used to identify various elements present in the interfacial region of the samples.

2.5. Thermomechanical analysis

Thermomechanical analysis was performed on monolithic magnesium and its composite using an automated SETARAM TMA 92-16.18 thermomechanical analyser that uses a spherical ended, 5 mm alumina probe to find the coefficients of thermal expansion (CTE) of the materials. The test was carried out in accordance with ASTM standard E831-00. Displacement of the monolithic magnesium and its composite samples were measured as a function of temperature (in the range of 50–400°C) and was subsequently used to determine the coefficient of thermal expansion. The temperature was measured by a K-type, coaxial thermocouple and argon

TABLE I Results of density and porosity measurements

Materials	Reinforcement 1 (Fe mesh) (vol%)	Reinforcement 1 (Fe mesh) (wt%)	Reinforcement 2 (Carbon fiber) (vol%)	Reinforcement 2 (Carbon fiber) (wt%)	Theoretical ρ(g/cm^3)	Experimental ρ(g/cm^3)	Porosity (%)
Mg	–	–	–	–	1.740	1.738 ± 0.002	0.12
Mg/Fe mesh/1 CF	3.0	12.0	0.071	0.066	1.919	1.896 ± 0.036	1.20

was used as the purge gas. Heating rate was maintained at 5°C/min. The experimental values of the CTE were correlated with those predicted by Rule-Of-Mixture (ROM) equation.

2.6. X-ray diffraction studies

X-Ray diffraction analysis was carried out on monolithic and composite samples using an automated Shimadzu LAB-X XRD-6000 X-ray diffractometer. Extruded and polished samples were exposed to Cu K_α radiation ($\lambda = 1.54056$ Å) using a scanning speed of 2 deg/min. The Bragg angles corresponding to different peaks were noted and the values of interplanar spacing, d obtained from the computerized output were subsequently compared and matched with the standard values for Mg, Fe, C and other related phases.

2.7. Mechanical characterization

The mechanical characterisation of the monolithic and composite specimens was carried out by performing microhardness, macrohardness and tensile tests. The microhardness test was conducted using a Matsuzawa MXT 50 digital microhardness tester with a Vickers indenter, using a test load of 25 gf and a dwell time of 15 s. Testing was performed in accordance with ASTM standard E384-99. Macrohardness of all specimens were measured using the Rockwell 15T Superficial Scale with a test load of 15 kgf and dwell time of 2 s. Hardness measurements were performed using a Future-Tech FR-3 Rockwell Type Hardness Tester in accordance with ASTM standard E18-02.

The tensile tests were conducted on round tension test specimens of 5 mm in diameter and 25 mm gauge length using an automated servohydraulic testing machine (Instron 8501). Tensile properties of the monolithic magnesium and composite materials were determined in accordance with ASTM standards E8M-01. Dynamic modulus of the specimens was determined based on measuring the dynamic elastic properties using the "free-free" or "suspended" beam method according to ASTM standard C1259-98.

2.8. Fracture behavior

Fracture surface characterization studies were performed on the tensile fractured surfaces of pure Mg and composite specimens in order to provide an insight into the various possible fracture mechanisms operative during the tensile loading of the samples. Fractography was accomplished utilizing a JEOL JSM-5600LV SEM.

3. Results

3.1. Macrostructure

The results of macrostructural characterization conducted on the as deposited ingots did not reveal any presence of macropores, blowholes or oxide sludge indicating the suitability of primary processing technique.

3.2. Density measurement

The results of the density measurements and porosity computations are given in Table I. The results indicate that near-dense monolithic and composite materials can be obtained using the fabrication methodology adopted in the present study. The results revealed that average porosity did not exceed 1.20% (see Table I).

3.3. Microstructural characterization

The results of image analysis on the size and aspect ratio of the grains for the monolithic and composites samples are shown in Table II. Scanning electron microscopy conducted on the extruded composite specimens showed good interfacial integrity between the matrix and the galvanized wire mesh (see Fig. 2). The interfacial integrity was assessed in terms of presence of microvoids and/or debonding.

Interfacial integrity between matrix and the carbon fibres was however not satisfactory. Microvoids were observed within the carbon fibre bundles and between the carbon fibres and the matrix indicating poor infiltration and wetting between magnesium and carbon fibres (see Fig. 2).

EDX analysis was conducted around the interfacial region and the results are summarized in Table III. Mg, Zn, Fe and O were consistently found in the iron wire-matrix interfacial region while Mg, Zn and O were found at the carbon fibre-matrix interfacial region.

3.4. Thermomechanical analysis

The results of CTE measurements obtained from monolithic and composite materials are shown in Table IV. The CTE predictions using ROM equation were also

TABLE II Results of grain size study

Materials	Vol fraction (%) Fe mesh	Vol fraction (%) C fiber	Grain size (μm)	Grain size G[a]	Aspect ratio
Mg	–	–	13 ± 1	9.5	1.9 ± 0.3
Mg/Fe mesh/1 CF	3.0	0.071	12 ± 4	9.5	1.5 ± 0.4

[a]Equivalent grain size number based on ASTM E112-96.

TABLE III Results of EDX analysis

		Elements present at			
		Reinforcement 1		Reinforcement 2	
Materials	Matrix	Iron mesh	Interface	Carbon fiber	Interface
Mg	Mg	–	–	–	–
Mg/Fe mesh/1 CF	Mg	Fe	Mg, Fe, Zn, O	C	Mg, Zn, O

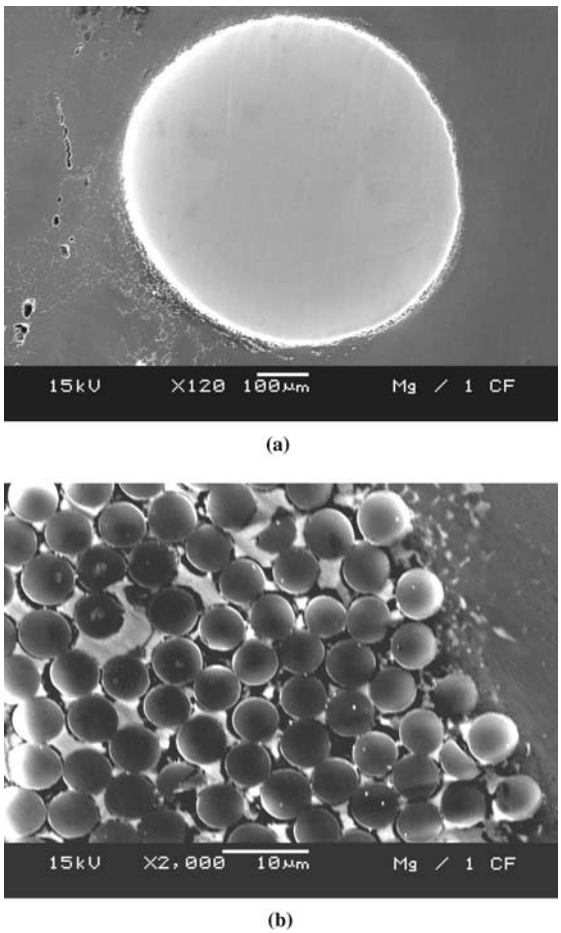

Figure 2 Representative SEM micrographs showing the interfacial integrity between (a) iron wire mesh and matrix, and (b) carbon fibers and matrix.

calculated for comparing with the experimentally obtained CTE values. It may be noted that the ROM model used in this study for comparing theoretical and experimental CTE values was originally developed for aligned continuous fibre reinforced composites. The ROM model is used in this present study since no theoretical models have been developed so far to predict the CTE of composites containing two types of continuous reinforcements which are interconnected and helical in nature.

TABLE IV Results of CTE measurements

		Theoretical CTE ($\times 10^{-6}$ /°C)	
Materials	Experimental CTE ($\times 10^{-6}$/°C)	Considering Zn[a]	Ignoring Zn[b]
Mg	29.05 ± 0.08	–	–
Mg/Fe mesh/1 CF	28.54 ± 0.75	28.65	28.62

[a]Theoretical CTE value calculated based on ROM was corrected for the presence of Zn, taking $\alpha_{Zn} = 39.7 \times 10^{-6}/K^{38}$ and $\alpha_{Fe} = 13.6 \times 10^{-6}/K^{38}$, $E_f = 188.822$ GPa.
[b]Theoretical CTE value based on ROM was calculated ignoring the presence of Zn, taking $\alpha_{Fe} = 13.6 \times 10^{-6}/K^{38}$, $E_f = 200$ GPa.

3.5. X-ray diffraction studies

The X-Ray diffraction results for the monolithic magnesium and the composite material are shown in Table V. Presence of carbon could not be traced in the XRD spectrum because of the limitation of filtered X-Ray radiation to detect phases with less than 2 vol% [29].

3.6. Mechanical behaviour

The results of macrohardness and microhardness measurements revealed significantly higher hardness values for the composite material when compared to the monolithic magnesium (see Table VI). The microhardness at the wire-matrix interface and the fibre-matrix interface were both higher when compared to the matrix region.

The results of the ambient temperature tensile testing are shown in Table VII. The results revealed that the presence of galvanized iron mesh and carbon fibres as reinforcements led to an increase in the dynamic modulus and 0.2%YS, did not affect the UTS and degraded the ductility of the magnesium matrix.

3.7. Fracture behaviour

Figs 3 to 5 shows the tensile fracture surface of magnesium and its composite. The fracture surface of the magnesium matrix reveals a typically brittle fracture with the presence of cleavage steps. For the composite specimens, presence of pullout of reinforcements, fibre breakage and circular cavities were additionally observed.

TABLE V Results of X-ray diffraction studies

	Reinforcement (Vol %)		No. of matching peaks	
Materials	Fe mesh	Carbon fibers	Mg	Fe
Mg	–	–	10[1]	–
Mg/Fe mesh/1 CF	3.0	0.071	9[2]	1[1]

[ ] represents the number of main peaks matched.

TABLE VI Results of macrohardness and microhardness measurements

Materials	Microhardness (HR15T)	Microhardness (HV)			
		Matrix	Fe mesh	Interface b/w Fe mesh and Mg	Interface b/w Carbon fiber and Mg
Mg	47 ± 1	41 ± 1	–	–	–
Mg/Fe mesh/1 CF	63 ± 5	51 ± 4	198 ± 8	132 ± 30	78 ± 12
Mg/Fe mesh[a]	–	48 ± 2	–	–	–

[a] Data obtained from reference [12].

TABLE VII Results of room temperature tensile properties

Materials	Reinforcements (vol%)		Elastic modulus *E* (GPa)	0.2% YS (MPa)	UTS (MPa)	Ductility (%)
Mg	–	–	39.8*	153 ± 8	228 ± 18	9.0 ± 1.5
Mg/Fe mesh/1 CF	3.0	0.071	42.5*	173 ± 4	224 ± 25	3.0 ± 1.4
Mg/Fe mesh[a]	5.1		49	141 ± 11	185 ± 30	2.6 ± 1.8
Mg/10 SiC[b]	10.0		45	120	160	2
Mg/10.3 SiC[c]	10.3	–	41.2	127 ± 7	195 ± 7	6.0
Mg/16.0 SiC[c]	16.0	–	43.6	120 ± 5	181 ± 6	4.7
Mg/21.3 SiC[c]	21.3	–	50.0	128 ± 2	176 ± 4	1.4
AZ91/SiC[d]	10.0		44.7	135	152	0.8

*Values obtained based on dynamic modulus testing according to ASTM C1259.
[a] Data obtained from reference [12].
[b] Data obtained from reference [40].
[c] Data obtained from reference [27].
[d] Data obtained from reference [5].

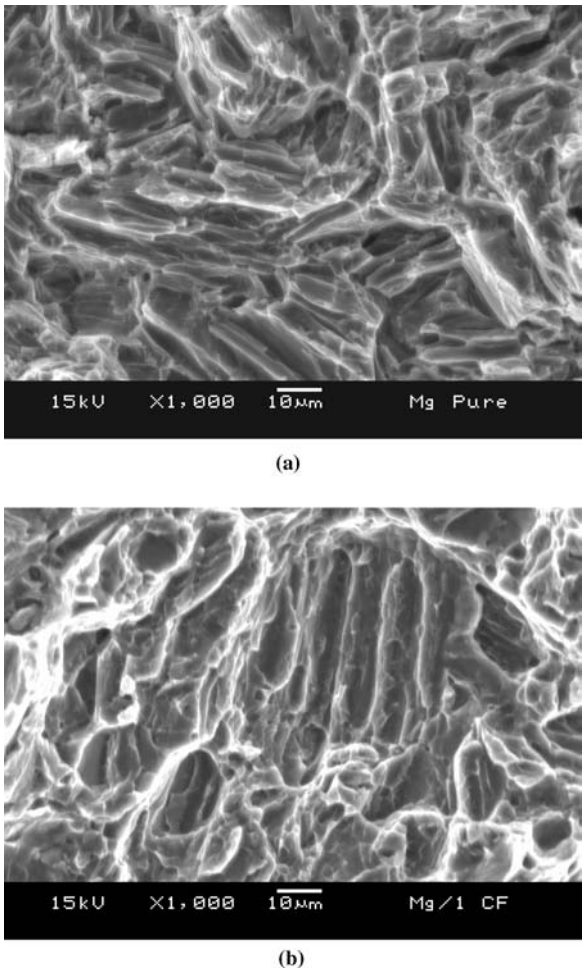

Figure 3 Representative SEM micrographs taken from the tensile fracture surface of: (a) pure Mg, and (b) matrix region for Mg/Fe mesh/1 CF.

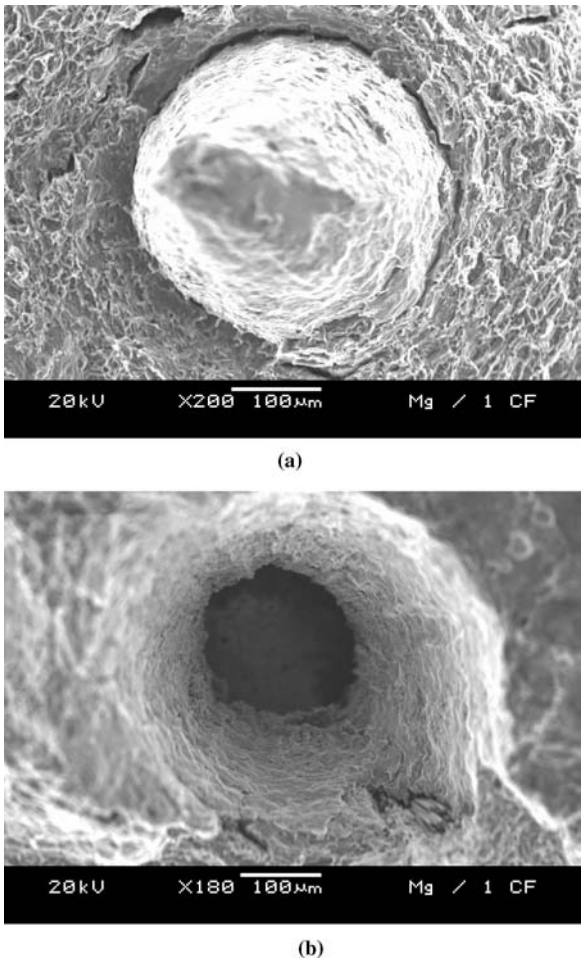

Figure 4 Representative SEM micrographs taken from the tensile fracture surface of hybrid composite showing the (a) debonding and fracture of Fe mesh from the matrix, and (b) circular cavity due to pullout of Fe mesh.

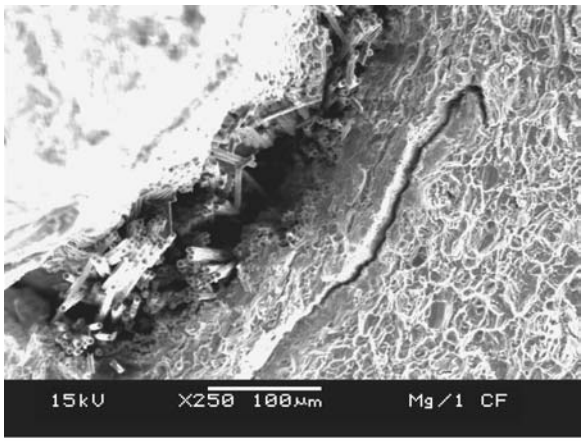

(a)

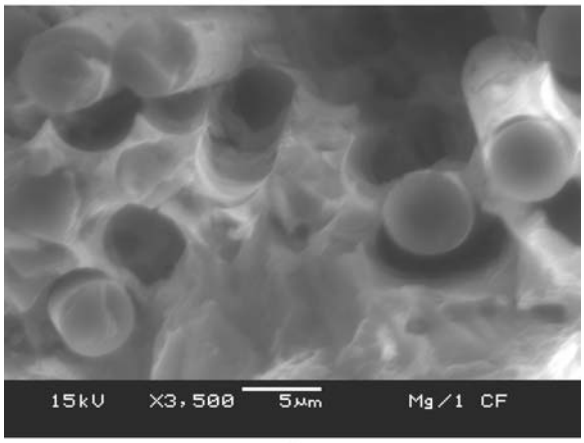

(b)

Figure 5 Representative SEM micrographs taken from the tensile fracture surface of composite showing: (a) pullout of carbon fibers, (b) pullout and debonding of carbon fibers from matrix.

4. Discussion

4.1. Synthesis of monolithic Mg and composite

Synthesis of magnesium-based composite containing two types of continuous reinforcement was successfully accomplished using the DMD process followed by hot extrusion. The absence of macropores and blowholes indicates adequate solidification conditions in the mould. It also demonstrates that the continuous flow of argon during the melting and deposition process did not lead to the entrapment of gases and there is no need to apply pressure to the solidifying melt to improve the infiltration [30, 31]. The results of density and porosity measurements indicated the capability of this fabrication methodology to synthesize near net shapes.

4.2. Microstructure

Microstructural characterization studies of extruded specimens revealed predominantly equiaxed grain structure indicating that the extrusion temperature chosen was sufficient to allow the recrystallization leading to the formation of strain-free grains during extrusion [32]. The grain sizes of the monolithic and composite samples were similar indicating that 3.071 volume percent of hybrid reinforcement was not sufficient to retard the growth of magnesium grain during solidification. The reduction in aspect ratio can be attributed to the ability of the reinforcement to minimize the directional growth of grains [33].

SEM micrographs revealed good interfacial integrity between matrix and iron mesh in the case of composite samples (see Fig. 2). Limited interfacial reaction was observed at the interface between the iron mesh and the matrix. Microvoids and porosity were minimal around the interface. The results are consistent with the results obtained on un-hybridized Mg/Fe mesh composites [12].

Interfacial integrity for matrix and carbon fibres was not satisfactory. Presence of voids was observed in-between carbon fibres (Refer to Fig. 2). This can be attributed to poor wettability of carbon fibres by the molten magnesium [16–20, 34, 35] and the roughness of the carbon fibre surface which may entrap gases that eventually lead to the formation of voids at the interface [35]. Mechanics of capillary and liquid metal flow helps to explain the presence of voids in-between the fibres [36, 37]. Studies by Rawal *et al*. [18] on the fibre-matrix interface of cast Gr/Mg found that electropositive magnesium is likely to be covered with an oxide layer which lowers wetting by preventing contact of metal with fibres and microvoids near the interface is primarily due to 23% contraction in volume involved during the formation of Mg_2Si and MgO from its element. High concentration of imperfections present at the interface may provide the nuclei for condensation of vacancies and accelerate microvoid formation. EDX analysis on the interface confirmed the presence of Mg and O (see Table III), indicating the likelihood of MgO formation. The presence of zinc detected is due to the zinc coating present on the wire mesh.

4.3. Physical behavior

The results of CTE measurement revealed that the incorporation of galvanized iron mesh and carbon fibres as reinforcement in the magnesium matrix reduced the average CTE of the magnesium matrix (see Table IV). The results demonstrated the ability of using hybrid reinforcement methodology to effectively constraint the longitudinal expansion of the matrix due to temperature variations. The average experimental CTE value was found to be lower than those theoretically predicted. This is consistent with the findings of other investigators [38, 39].

4.4. Mechanical behaviour

Results of macrohardness measurements revealed that the addition of reinforcements increased the hardness of the composite by ∼34% when compared to the monolithic magnesium (see Table VI). This can primarily be attributed to the presence of iron mesh and carbon fibres as reinforcements. Microhardness measurements conducted at the matrix revealed that the presence of reinforcement leads to an increase in the microhardness of the matrix by ∼24% compared to the monolithic magnesium matrix. Higher hardness exhibited by composite samples can be attributed to the: (a) presence of harder

reinforcements in the matrix and (b) higher constraint to the localized matrix deformation due to the presence of the reinforcements. These results are also consistent with the observation of other researchers [21].

Hardness measurements conducted at the reinforcement/matrix interface revealed two things: (a) hardness of the interface remains distinctly superior when compared to matrix hardness and (b) hardness of Fe/Mg interface was superior to that of C/Mg interface. The higher hardness of the interfacial region, in general, can be attributed to the CTE mismatch between reinforcements and the matrix resulting in an increase in defect concentration at the interface (such as dislocation density) that allows for the solid solution/precipitation strengthening of the interfacial area. The superior hardness of Fe/Mg interface can be attributed to: (a) almost defect free interface (see Fig. 2), (b) dissolution of zinc in magnesium (see Table III) and (c) possibility of interfacial reaction between Mg and Zn. All these three factor were either absent or minimal in the case of C/Mg interface.

The results of tensile properties characterization revealed that the coupled use of galvanized iron mesh and carbon fibres as reinforcements led to an increase in dynamic modulus and 0.2%YS, did not affect the ultimate tensile strength and degrades the ductility. The increase in dynamic modulus for reinforced magnesium was expected and can primarily be attributed to the presence of high modulus reinforcements ($E_{\mathrm{Fe}} = 200$ GPa; $E_{\mathrm{Carbon}} = 276$ GPa). The increase in 0.2%YS can be ascribed to the coupled presence of carbon fibres and galvanized iron mesh. In earlier studies [12], it was observed that the addition of wire mesh alone and even in comparatively higher volume fraction does not affect the yield strength (see Table VII). The results of the present study also indicate that the UTS of the hybrid magnesium composite remained similar to that of pure magnesium. The results are encouraging as the UTS was always found to degrade in the case of magnesium based composites containing either continuous [12] or discontinuous [27] reinforcements. The improvement in strength in the case of hybrid composites when compared to work of other researchers [5, 12, 27, 40] can also be attributed to the development of cellular dislocation and twins substructure as suggested by researchers elsewhere [22]. Further work is continuing to establish this hypothesis for the composite synthesized in the present study.

The results of mechanical properties characterization, in essence, revealed that a superior combination of hardness and tensile properties can be realised in the hybrid composites (such as Mg/Fe mesh/1CF composite) when compared to conventional composites with one type of reinforcement (see Tables VI and VII).

4.5. Fracture behaviour

The results of fracture analysis revealed typical brittle fracture in the case of magnesium samples (see Fig. 3). This can be attributed to the HCP crystal structure of the magnesium, which restricts the slip to the basal plane. The presence of small steps and microscopically rough fracture surface indicates the inability of magnesium to cleave on any single plane. The fracture surface features of pure magnesium and that of magnesium matrix in the case of composite remained similar (see Fig. 3).

The results of fractographic studies conducted on the hybrid composite revealed the presence of pulled-out mesh and circular cavities (see Fig. 4). These indicate that under uniaxial tensile loading, crack initiation and/or propagation was facilitated through the matrix-wire interfacial region. The presence of shallow rather than deep circular cavities indicate the possibility of failure of interconnections followed by the pullout of wire or partial damage of the interconnections during extrusion and subsequent pullout of the wire as a result of relatively weak interfacial zone. Fracture surfaces at the tip of exposed wire indicate a ductile mode of failure with an apparent reduction in cross-sectional area of the wire (see Fig. 4). These indicate the ability of the matrix to transfer load to the wire mesh reinforcement. Interfacial debonding of wire mesh was also observed on the fractured samples of synthesized composites (see Fig. 4a). Similar features (debonding, breakage and pull-out) were noticed for carbon fibres except that the fractured carbon fibres' surface was flat (see Fig. 5).

5. Conclusions

The main conclusions derived from this study are as follows:

(1) DMD technique followed by hot extrusion can be effectively used for the synthesis of hybrid magnesium composite containing two types of continuous reinforcement.

(2) The addition of galvanized iron wire mesh and carbon fibres lead to marginal improvement in CTE of the elemental magnesium.

(3) The use of hybrid reinforcement methodology lead to an improvement in the overall combination of hardness and tensile properties when compared to monolithic magnesium and conventional Mg/SiC and Mg/Fe mesh formulations containing comparatively higher volume percentages of one type of reinforcement.

Acknowledgements

The authors would like to thank NUS (grant #R-265-000-142-112) for financial support and Mr. Narasimalu Srikanth, located at ASM Technology, Singapore for his help in determining the dynamic modulus of the unreinforced and reinforced magnesium specimens.

References

1. H. P. DEGISCHER, M. DOKTOR and P. PRADER, in "Metal Matrix Composites and Metallic Foams", edited by T. W. Clyne *et al.*, "Euromat 99" (Wiley-VCH, Weinheim, 2000) Vol. 5, p. 113.
2. B. TERRY and G. JONES, in "Metal Matrix Composites: Current Developments and Future Trends in Industrial Research and Applications" (Elsevier Advanced Technology, Oxford, 1990) p. 41.
3. V. LAURENT, P. JARRY, G. REGAZZONI and D. APELIAN, *J. Mater. Sci.* **27** (1992) 4447.

4. D. J. LLYOD, *Int. Mater. Rev.* **39** (1994) 1.
5. A. LUO, *Metal. Mater. A* **26** (1995) 2445.
6. D. M. LEE, B. K. SUH, B. G. KIM, J. S. LEE and C. H. LEE, *Mater. Sci. Technol.* **13** (1997) 590.
7. T. EBERT, F. MOLL and K. U. KAINER, *Powder Metal.* **40** (1997) 126.
8. D. J. TOWLE and C. M. FRIEND, *Mater. Sci. Eng. A* **188** (1994) 153.
9. R. UNVERRICHT, V. PEITZ, W. RIEHEMANN and H. FERKEL, in "Magnesium Alloys and their Applications" (Werkstoff-Informationsgesellschaft mbH, Germany, 1998) p. 327.
10. I. W. HALL, *J. Mater. Sci.* **26** (1991) 776.
11. M. RUSSELL-STEVENS, D. C. PLANE, J. SUMMERSCALES, P. SCHULZ and M. PAPAKYRIACOU, *Mater. Sci. Technol.* **18** (2002) 501.
12. V. V. GANESH and M. GUPTA, *Mater. Res. Bull.* **35** (2000) 2275.
13. S. F. HASSAN and M. GUPTA, *Mater. Res. Bull.* **37** (2002) 337.
14. S. F. HASSAN and M. GUPTA, *J. Alloy Compd.* **335** (2002) 10.
15. S. F. HASSAN and M. GUPTA, *J. Alloy Compd.* **345** (2002) 246.
16. R. CHEN and X. LI, *Compos. Sci. Technol.* **49** (1993) 357.
17. R. WU, in "Composite Interfaces (ICCI-II)" (Elsevier Science Publishing, Cleveland, Ohio, 1988) p. 43.
18. S. P. RAWAL and M. S. MISRA, in "Composite Interfaces (ICCI-II)" (Elsevier Science Publishing, Cleveland, Ohio, 1988) p. 179.
19. P. SCHULZ, H. KAUFMANN and H. CAPEL, in "Metal Matrix Composites and Metallic Foams", edited by T. W. Clyne *et al*., Euromat 99 (Wiley-VCH, Weinheim, 2000) Vol. 5 p. 128.
20. M. OTTMULLER, C. KORNER and R. F. SINGER, in "Metal Matrix Composites and Metallic Foams", edited by T. W. Clyne *et al*., Euromat 99 (Wiley-VCH, Weinheim, 2000) Vol. 5, p. 168.
21. J. SCHRODER and K. U. KAINER, *Mater. Sci. Eng. A* **135** (1991) 33.
22. F. WU, J. ZHU, Y. CHEN and G. ZHANG, *Mater. Sci. Eng. A* **277** (2000) 143.
23. T. W. CHOU, in "Microstructural Design of Fiber Composites" (Cambridge University Press, Cambridge, New York, 1993) p. 231.
24. Hexcel Fibers website, IM7 HS-CP5000 Carbon Fiber Product Data, http://www.hexcelfibers.com/Tools/Downloads/default.htm (accessed Sept. 2004).
25. M. GUPTA, M. O. LAI and C. Y. SOO, *Mater. Res. Bull.* **30** (1995) 1525.
26. M. GUPTA, L. M. THAM and L. CHENG, *Mater. Sci. Technol.* **15** (1999) 1139.
27. M. GUPTA, M. O. LAI and D. SARAVANARANGANTHAN, *J. Mater. Sci.* **35** (2000) 2155.
28. M. GUPTA, C. LANE and E. J. LAVERNIA, *Scr. Metall. Mater.* **26** (1992) 825.
29. B. D. CULLITY, in "Elements of X-ray Diffraction", 2nd edn (Addison-Wesley, Reading, MA, 1978) p. 414.
30. R. K. EVERETT and R. J. ARSENAULT, in "Metal Matrix Composites" (Academic Press Publishers, Boston, 1991) p. 64.
31. R. ASTHANA, *J. Mater. Synth. Proces.* **5** (1997) 251.
32. M. GUPTA, L. SU and T. S. SRIVATSAN, *Revi. Proc. Chem. Engng.* **1** (1998) 179.
33. M. GUPTA, M. O. LAI and M. S. BOON, *Mater. Res. Bull.* **33** (1998) 1387.
34. B. L. MORDIKE and P. LUKAC, *Surf Interf. Anal.* **31** (2001) 682.
35. S. P. RAWAL, *Surf Interf. Anal.* **31** (2001) 692.
36. A. MORTENSEN, *Mater. Sci. Eng. A* **135** (1991) 1.
37. J. JACKOWSKI, in "Metal Matrix Composites and Metallic Foams", edited by T. W. Clyne *et al*., Euromat 99 (Wiley-VCH, Weinheim, 2000) Vol. 5, p. 133.
38. V. V. GANESH, P. K. TAN and M. GUPTA, *J. Alloy Compd.* **315** (2001) 203.
39. L. TAO and F. DELANNAY, *Acta Mater.* **46** (1998) 6497.
40. M. R. KRISHNADEV, R. ANGERS, C. G. KRISHNADAS NAIR and G. J. HUARD, *J. Mater.* **45** (1993) 52.

Received 18 October
and accepted 22 December 2004